Structural Engineering and Mechanics, Vol. 12, No. 4 (2001) 409-428 409
DOI: http://dx.doi.org/10.12989/sem.2001.12.4.409

Computer simulation for dynamic wheel loads of heavy vehicles

Mitsuo Kawatani†

Department of Civil Engineering, Kobe University, 1-1 Rokkodai-Cho, Nada-gu, Kobe 657-8501, Japan

Chul-Woo Kim‡

Department of Civil Engineering, Pohang College, 55 Jukchun-Dong, Buk-gu, Pohang 791-711, Korea

Abstract. The characteristics of dynamic wheel loads of heavy vehicles running on bridge and rigid surface are investigated by using three-dimensional analytical model. The simulated dynamic wheel loads of vehicles are compared with the experimental results carried out by Road-Vehicles Research Institute of Netherlands Organization for Applied Scientific Research (TNO) to verify the validity of the analytical model. Also another comparison of the analytical result with the experimental one for Umeda Entrance Bridge of Hanshin Expressway in Osaka, Japan, is presented in this study. The agreement between the analytical and experimental results is satisfactory and encouraging the use of the analytical model in practice. Parametric study shows that the dynamic increment factor (DIF) of the bridge and RMS values of dynamic wheel loads are fluctuated according to vehicle speeds and vehicle types as well as roadway roughness conditions. Moreover, there exist strong dominant frequency resemblance between bounce motion of vehicle and bridge response as well as those relations between RMS values of dynamic wheel loads and dynamic increment factor (DIF) of bridges.

Key words: dynamic increment factor (DIF); dynamic wheel load; Power spectral density (PSD); Root mean square (RMS); three-dimensional dynamic analysis; traffic-induced vibration.

1. Introduction

Dynamic response of bridges caused by vehicle loading is one of the major dynamic phenomena because the applied loads varied with time (Mulcathy 1983). Furthermore, the pavement deterioration is also affected by time-varying vehicle loads. Therefore, it has been a main subject in bridge and pavement engineering to devise numerical model or simulation method which can estimate the dynamic wheel loads rationally.

To improve the understanding about dynamic responses of the bridge actuated by moving vehicle, many research works have been carried out using analytical and experimental methods (Huang 1976, Cantieni 1992). More recent researches on bridge-vehicle interaction can be categorized under seven headings (Fafard *et al.* 1993); the effects of bridge span lengths, the effects of suspension systems, the effects of braking, the effects of axle spacing, the effects of highway road roughness,

† Professor
‡ Lecturer

the effects of load speed, mass and bridge damping, and the effects of gross vehicle weight.

Such an analytical approach for this dynamic response of bridges as the two-dimensional model gives good analytical results for bridge responses (Yang *et al.* 1997). However, these two-dimensional investigations cannot estimate dynamic responses of deck slabs and local members in the bridge system (Kawatani and Kim 1998). Moreover, in view of the riding comfort of vehicles running on bridge and roadway, two-dimensional vehicle model cannot consider the vehicle-motion like rolling and axle tramp which also contribute the riding comfort of vehicles.

A few three-dimensional analytical models for the vehicle and bridge thus have been developed, but most of these former works have been focused on only bridge responses. What is worse, there is little verification with experimental results when considering dynamic wheel loads of vehicles. In this study, therefore, the characteristics of the dynamic wheel loads of the heavy vehicles are investigated using developed simulation method.

To verify the validity of the analytical model presented, comparative studies on dynamic wheel loads and bridge responses with experimental results are carried out. The concept of root mean square (RMS) values and dynamic increment factor (DIF) (Kawatani *et al.* 1993) is used to investigate the correlation between analytical and experimental results of the dynamic wheel loads of vehicle and dynamic responses of bridges, respectively.

As parametric study, the effects of vehicle speed to dynamic features of the wheel loads and bridge responses as well as those effects on frequency relations between dynamic wheel loads and bridge responses are investigated. The relationships between vehicle motion or dynamic wheel load and dynamic responses of bridges are also examined.

2. Equations of forced vibration for bridge-vehicle interaction

To develop equation of motion for bridge, finite element method (FEM) and modal analysis are adopted. Girder system and lateral bracing are idealized as beam element with 6 DOF at each node and the deck slab is idealized as four nodes plate element with Lagrange polynomials (Zienkiwicz and Taylor 1991). The lumped mass system and Rayleigh damping (Agabein 1971) are adopted to form mass and damping matrices of the bridge model, respectively.

The normalized dynamic equation of motion for the bridge can be written as Eq. (1).

$$[\bar{M}_b]\{\ddot{a}\} + [\bar{C}_b]\{\dot{a}\} + [\bar{K}_b]\{a\} = \{\bar{f}\} \tag{1}$$

where, $[\bar{M}_b]=[\Phi]^T[M_b][\Phi]$, $[\bar{C}_b]=[\Phi]^T[C_b][\Phi]$, $[\bar{K}_b]=[\Phi]^T[K_b][\Phi]$ and $\{\bar{f}\}=[\Phi]^T\{f\}$. The matrices $[M_b]$, $[C_b]$ and $[K_b]$ are mass, damping and stiffness matrices of bridge respectively, and load vector $\{f\}$ is the dynamic wheel load generated by vehicle running on bridge with roadway roughness. $[\Phi]$ and $\{a\}$ denote modal matrix and normal coordinate vector of the bridge deflection. The generalized deflection and external force vector of the bridge are shown in Eq. (2) and Eq. (3), respectively.

$$\{w\}=\sum_{i}^{n}\{\phi_i\}a_i = [\Phi]\{a\} \tag{2}$$

$$\{f\}=\sum_{m=1}^{3}\sum_{u=1}^{2}\{\Psi_{mu}\}P_{mu}(t) \tag{3}$$

where, $\{\phi_i\}$ and a_i are the mode vector and the normal coordinate of the bridge deflection at ith mode respectively. $\{\Psi_{mu}\}$ is the load distribution vector to deliver a wheel load on the bridge deck to each node of the plate element. m indicates tire location, for example m=3 indicates the rear tire of rear axle in Fig. 1, and u indicates left or right wheel. The dynamic wheel load vector $P_{mu}(t)$ will be explained later.

To derive dynamic equations of motion for the bridge-vehicle interaction, it is necessary to formulate equations of motion for three-dimensional vehicle model. The idealized vehicle model of a heavy dump truck with one front and two rear axles is a system with 8 degrees of freedom (8 DOF) as shown in Fig. 1. The sprung and unsprung masses are connected by a set of linear springs and dashpots. The friction in the vehicle suspension system is not considered.

In Fig. 1, m_v, K_v, C_v, Z and θ express mass, spring constant, damping coefficient, displacement and rotational angle of vehicle, respectively. Z_{11}, Z_{12}, Z_{22}, θ_{x11}, θ_{x12}, θ_{x22}, θ_{y11} and θ_{y22} express bounce, parallel hop of front axle, parallel hop of rear axle, rolling, axle tramp of front axle, axle tramp of rear axle, pitching and axle windup motion of each part of the vehicle system, respectively.

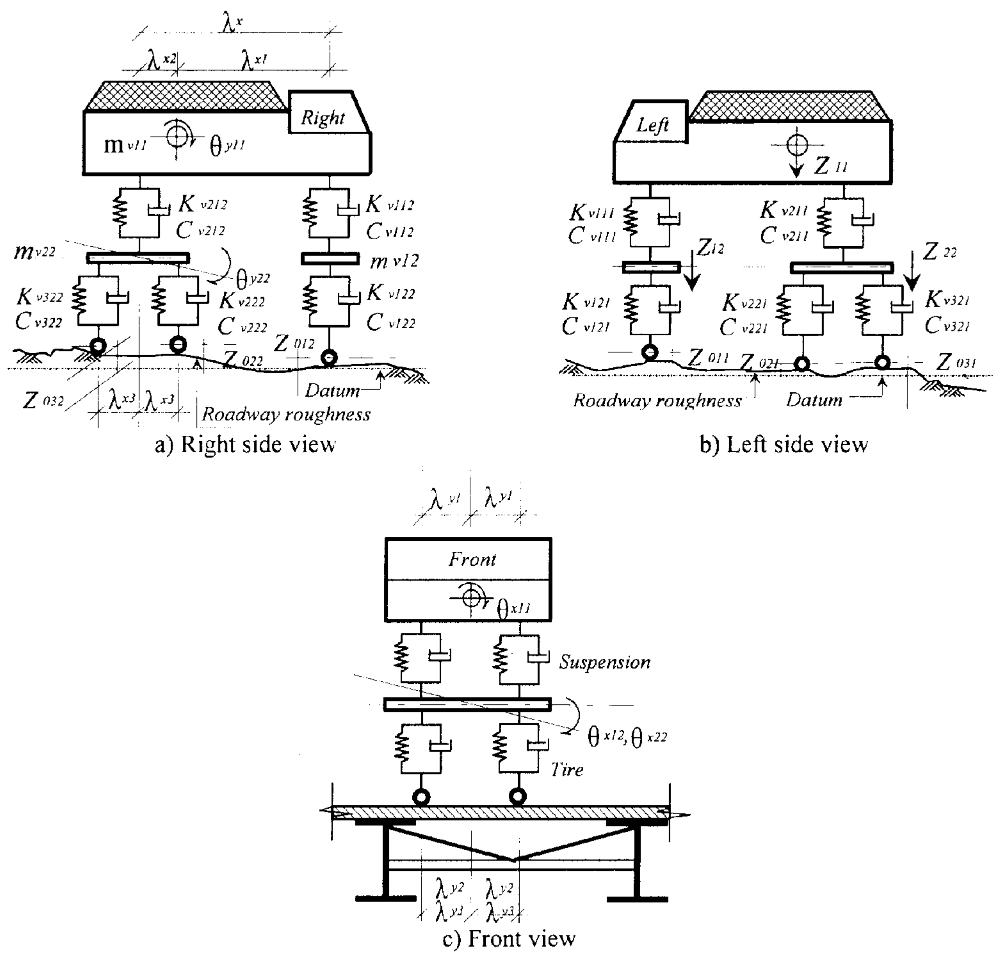

Fig. 1 Idealization of heavy dump truck

Lagrange equation of motion expressed in Eq. (4) is adopted to derive dynamic equations of motion for 8 DOF vehicle system.

$$\frac{\partial}{\partial t}\left(\frac{\partial T}{\partial \dot{q}_i}\right) - \frac{\partial T}{\partial q_i} + \frac{\partial U_e}{\partial q_i} + \frac{\partial U_d}{\partial \dot{q}_i} = 0 \tag{4}$$

where, T is the kinetic energy of the system, U_e is the potential energy of the system by elastic motion, U_d is dissipation energy of the system by damping and q_i is the ith generalized co-ordinate.

The final dynamic equations of motion for vehicle can be summarized as follows according to Eq. (4).

$$m_{v11}\ddot{Z}_{11} + \sum_{s=1}^{2}\sum_{u=1}^{2} v_{s1u}(t) = 0 \tag{5}$$

$$m_{v12}\ddot{Z}_{12} - \sum_{u=1}^{2} v_{11u}(t) + \sum_{u=1}^{2} v_{12u}(t) = 0 \tag{6}$$

$$m_{v22}\ddot{Z}_{22} - \sum_{u=1}^{2} v_{21u}(t) + \sum_{m=2}^{3}\sum_{u=1}^{2} v_{m2u}(t) = 0 \tag{7}$$

$$m_{v11}\lambda_{y1}^2\ddot{\theta}_{x11} - \sum_{s=1}^{2}\sum_{u=1}^{2}(-1)^u\lambda_{y1}v_{s1u}(t) = 0 \tag{8}$$

$$m_{v12}\lambda_{y2}^2\ddot{\theta}_{x12} + \sum_{u=1}^{2}(-1)^u\lambda_{y2}v_{11u}(t) - \sum_{u=1}^{2}(-1)^u\lambda_{y2}v_{12u}(t) = 0 \tag{9}$$

$$m_{v22}\lambda_{y3}^2\ddot{\theta}_{x22} + \sum_{u=1}^{2}(-1)^u\lambda_{y3}v_{21u}(t) - \sum_{m=2}^{3}\sum_{u=1}^{2}(-1)^u\lambda_{y3}v_{m2u}(t) = 0 \tag{10}$$

$$m_{v11}\lambda_{x1}\lambda_{x2}\ddot{\theta}_{y11} - \sum_{s=1}^{2}\sum_{u=1}^{2}(-1)^s\lambda_{xs}v_{s1u}(t) = 0 \tag{11}$$

$$m_{v22}\lambda_{x3}^2\ddot{\theta}_{y22} + \sum_{m=1}^{3}\sum_{u=1}^{2}(-1)^m\lambda_{x3}v_{m2u}(t) = 0 \tag{12}$$

where,

$$v_{s1u}(t) = K_{vs1u}\begin{Bmatrix} Z_{11}-(-1)^s\lambda_{xs}\theta_{y11}-(-1)^u\lambda_{y1}\theta_{x11} \\ -Z_{s2}+(-1)^u\lambda_{y(s+1)}\theta_{xs2} \end{Bmatrix} + C_{vs1u}\begin{Bmatrix} \dot{Z}_{11}-(-1)^s\lambda_{xs}\dot{\theta}_{y11}-(-1)^u\lambda_{y1}\dot{\theta}_{x11} \\ -\dot{Z}_{s2}+(-1)^u\lambda_{y(s+1)}\dot{\theta}_{xs2} \end{Bmatrix} \tag{13}$$

$$v_{12u}(t) = K_{v12u}\{Z_{12}-(-1)^u\lambda_{y2}\theta_{x12}-Z_{01u}\} + C_{v12u}\{\dot{Z}_{12}-(-1)^u\lambda_{y2}\dot{\theta}_{x12}-\dot{Z}_{01u}\} \tag{14}$$

$$\begin{aligned} v_{m2u}(t) = {} & K_{vm2u}\{Z_{22}+(-1)^m\lambda_{x3}\theta_{y22}-(-1)^u\lambda_{y3}\theta_{x22}-Z_{0mu}\} \\ & + C_{vm2u}\{\dot{Z}_{22}+(-1)^m\lambda_{x3}\dot{\theta}_{y22}-(-1)^u\lambda_{y3}\dot{\theta}_{x22}-\dot{Z}_{0mu}\} \quad (m=2,\ 3) \end{aligned} \tag{15}$$

The subscripts used above equations are summarized in Table 1. Z_{0mu} is the relative displacement between deflection of bridge and roadway roughness as shown in Eq. (16), and also Fig. 2

Table 1 Subscripts

Subscript	Meaning	Remarks
b	bridge	K_b : stiffness of bridge
v	vehicle	K_v : stiffness of vehicle
s	suspension	s=1 : front suspension of vehicle s=2 : rear suspension of vehicle
m	tire	m=1 : tire at front axle of vehicle m=2 : front tire at rear axle of vehicle m=3 : rear tire at rear axle of vehicle
u	left and right	u=1 : left part of vehicle u=2 : right part of vehicle

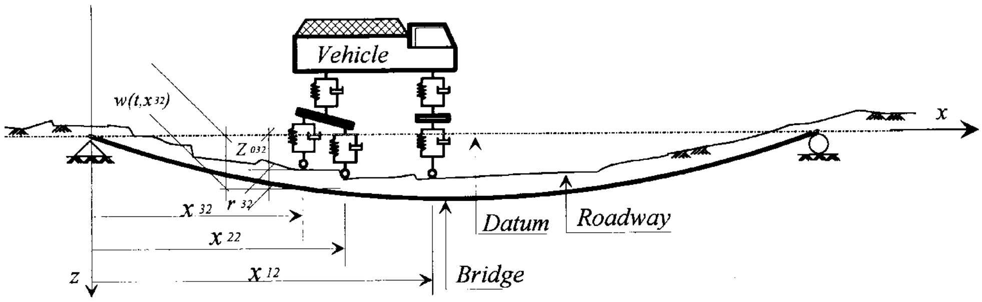

Fig. 2 Scheme for relative displacement

(Mulcathy 1983) shows the scheme for Z_{0mu}.

$$Z_{0mu} = w(t,x_{mu}) - r_{mu} \tag{16}$$

$$w(t,x_{mu}) = \{\Psi\}^T_{mu}[\Phi]\{a\} \tag{17}$$

where, $w(t,x_{mu})$ denotes the deflection of bridge at time t and position x_{mu} as shown in Fig. 2, and it is defined in Eq. (17) using the load distribution vector $\{\Psi\}_{mu}$. r_{mu} denotes roadway roughness at x_{mu}. v_{m2u} (m=1, 2, 3) written in Eqs. (13), (14) and (15) indicates dynamic force according to vehicle running on bridge with roadway roughness, therefore the dynamic wheel load which activate bridge vibration can be calculated by considering weight of vehicle and dynamic force (Inbahathan and Wieland 1987). Thus expression for dynamic wheel load at each wheel that located at x_{mu} from starting position can be written as Eq. (18) and Eq. (19)

$$\begin{aligned} P_{1u}(t) &= \frac{1}{2}\left(1-\frac{\lambda_{x1}}{\lambda_x}\right)m_{v11}g + \frac{1}{2}m_{v12}g + v_{12u}(t) = \frac{1}{2}\left(1-\frac{\lambda_{x1}}{\lambda_x}\right)m_{v11}g + \frac{1}{2}m_{v12}g \\ &+K_{v12u}\left\{ Z_{12} - (-1)^u\lambda_{y2}\theta_{x12} - \left(\{\Psi_{1u}(t)\}^T[\Phi]\{a\} - r_{1u}\right)\right\} \\ &+ C_{v12u}\left\{ \dot{Z}_{12} - (-1)^u\lambda_{y2}\dot{\theta}_{x12} - \left(\{\Psi_{1u}(t)\}^T[\Phi]\{\dot{a}\} - \dot{r}_{1u}\right)\right\} \end{aligned} \tag{18}$$

$$P_{mu}(t) = \frac{1}{4}\left(1 - \frac{\lambda_{x2}}{\lambda_x}\right)m_{v11}g + \frac{1}{4}m_{v22}g + v_{m2u}(t) = \frac{1}{4}\left(1 - \frac{\lambda_{x2}}{\lambda_x}\right)m_{v11}g + \frac{1}{4}m_{v22}g \quad (m=2,\ 3)$$
$$+ K_{vm2u}\left\{ Z_{22} + (-1)^m \lambda_{x3}\theta_{y22} - (-1)^u \lambda_{y3}\theta_{x22} - \left(\{\Psi_{mu}(t)\}^T[\Phi]\{a\} - r_{mu}\right)\right\}$$
$$+ C_{vm2u}\left\{ \dot{Z}_{22} + (-1)^m \lambda_{x3}\dot{\theta}_{y22} - (-1)^u \lambda_{y3}\dot{\theta}_{x22} - \left(\{\Psi_{mu}(t)\}^T[\Phi]\{\dot{a}\} - \dot{r}_{mu}\right)\right\} \quad (19)$$

where, g means gravity acceleration, and $\{\Psi_{mu}(t)\}^T[\Phi]\{a\} - r_{mu}$ expresses relative displacement between bridge deflection and roadway roughness as defined in Eqs. (16) and (17).

The final dynamic equations for bridge-vehicle interaction system with roadway roughness can be derived using Eq. (1) and Eqs. (5)-(12). By neglecting the Eq. (11) and elements related to θ_{y22} as well as substituting 1/2 into 1/4 of Eq. (19), the derived equations of motion can be applied to 7 DOF vehicle system. In addition, by neglecting matrices and variables related to bridge response, the equations also can be applied to the case of vehicle running on rigid surface. The simultaneous differential equations are solved using Newmark-β method as direct integration method.

In this study, the sign is taken as positive if the direction of displacement is downward, the pitching is occurred from rear to front suspension and the rolling is generated from the right to the left.

3. Bridge, vehicle and roadway roughness model

A steel plate girder bridge designated as medium span bridge with span length of 40.4 m and prestressed concrete bridge designated as short span bridge with span length of 18.8 m are used as numerical examples as shown in Fig. 3 and Fig. 4, respectively. The first and second fundamental natural frequencies of the medium span bridge are 2.34 Hz and 3.89 Hz respectively. Those natural frequencies of the short span bridge are 4.69 Hz and 6.65 Hz, respectively.

For vehicle models, 7 DOF model with gross weight of 161.8 kN and axle spacing of 6.2 m and 8 DOF model with gross weight of 190.8 kN and axle spacing of 3.99 m are used. The measured properties of each vehicle model are appeared in Table 2.

The measured roadway profiles shown in Fig. 5 and Fig. 6 are used in analysis, and each roadway profile is designated as Smooth Canadian Road (SCR) and Umeda Entrance Road (UER) respectively.

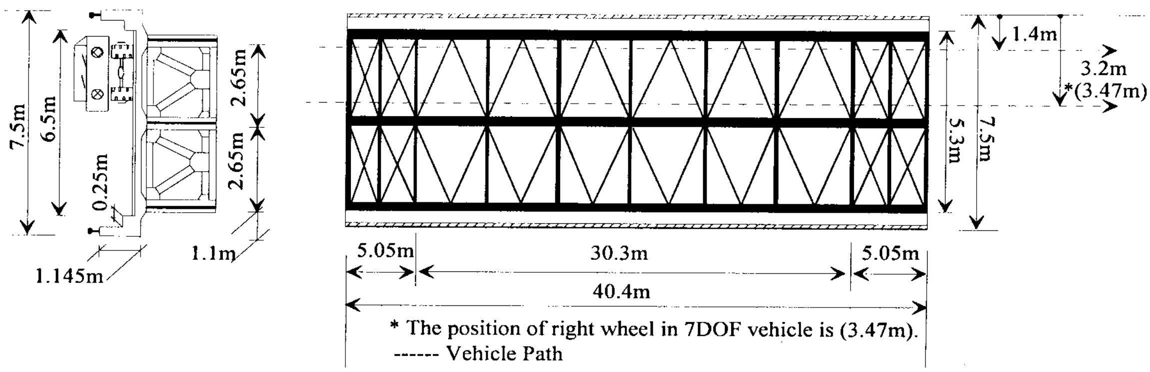

Fig. 3 Steel plate girder bridge (medium span)

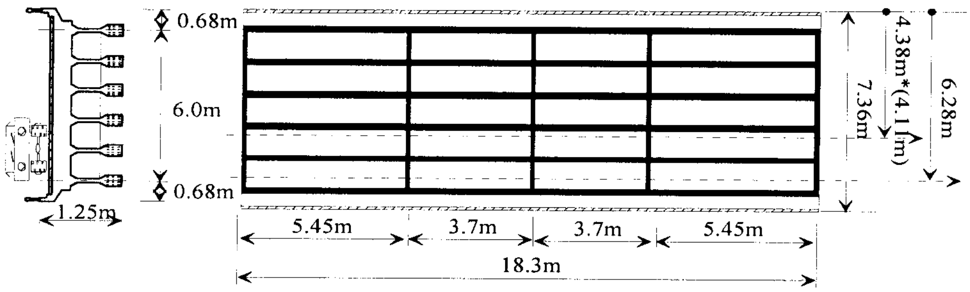

Fig. 4 Prestressed concrete bridge (short span)

Table 2 Properties of the vehicle systems

	Vehicle system / Property	7 DOF	8 DOF
Mass (kg)	m_{v11}	14790	18500
	m_{v12}	650	500
	m_{v21}	1070	1450
Stiffness (kN/m)	$K_{v111} = K_{v112}$	4760	1577
	$K_{v211} = K_{v212}$	1820	4724
	$K_{v121} = K_{v122}$	1390	3146
	$K_{v221} = K_{v222}$	1170	4724
	$K_{v321} = K_{v322}$	–	4724
Damping (kN.s/m)	C_{v111}	7.810	11.20
	C_{v112}	8.065	11.20
	C_{v211}	3.324	33.42
	C_{v212}	1.649	33.42
	$C_{v121} = C_{v122}$	–	13.30
	$C_{v221} = C_{v222} = C_{v321} = C_{v322}$	–	20.00
Geometry (m)	λ_x	6.20	3.99
	λ_{x1}	3.94	2.99
	λ_{x2}	2.26	1.00
	λ_{x3}	–	0.66
	λ_{y1}	1.04	0.90
	λ_{y2}	1.04	0.90
	λ_{y3}	0.96	0.93

According to ISO estimate (ISO 1971) based on the riding comfort of vehicle, it can be seen that the conditions of the roadway profiles are categorized as 'very smooth' or 'smooth' by comparison of power spectral density (PSD) curves shown in Figs. 7 and 8. In other words, it means that UER profile has relatively worse surface condition than that of SCR profile.

4. Verification of the analytical models

It will be useful to explain the nomenclatures used in this study before proceeding the discussion. **FL**, **FR**, **RL** and **RR** mean **F**ront **L**eft, **F**ront **R**ight, **R**ear **L**eft and **R**ear **R**ight wheel, respectively.

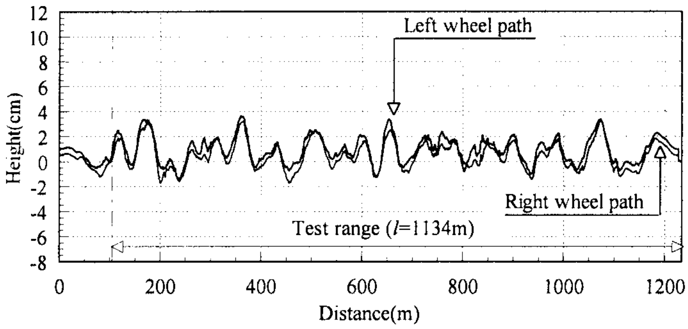

Fig. 5 Smooth Canadian Roadway profile (SCR profile)

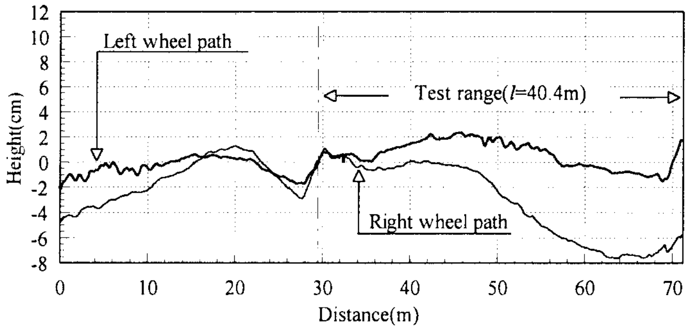

Fig. 6 Umeda Entrance Roadway profile (UER profile)

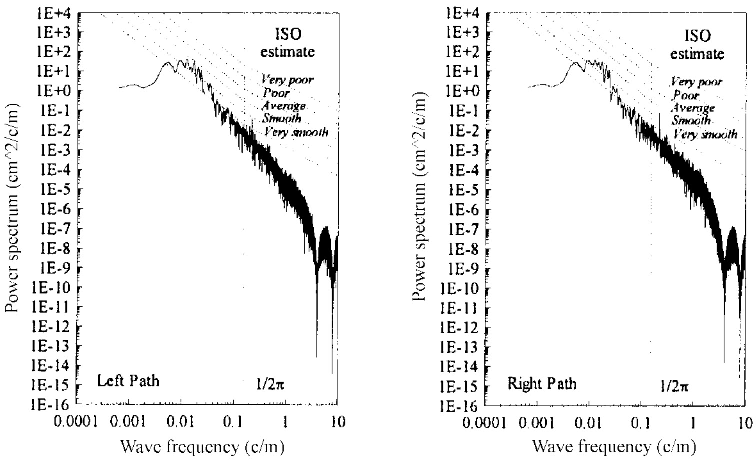

a) Left path b) Right path

Fig. 7 PSD curves of SCR profile

The **EXP** and **ANAL** express **Exp**erimental and **Anal**ytical results, respectively. For **7SSFR-R**, **7** and **SS** indicate **7** DOF vehicle system, **S**CR profile and length of **S**hort span bridge as running distance. **FR** and **–R** of **7SSFR-R** express **F**ront **R**ight wheel and **R**igid surface to indicate the case of running on road. Similarly, **8** and **UM** of **8 UMRRL-B** mean **8** DOF vehicle system, **U**ER

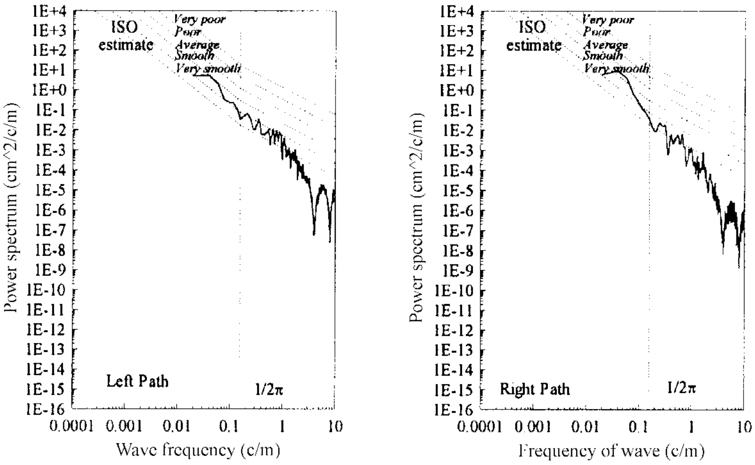

a) Left path b) Right path

Fig. 8 PSD curves of UER profile

profile and length of **M**edium span bridge as running distance. **RRL** and **-B** of **8 UMRRL-B** express **R**ear axle's **R**ear **R**ight wheel and **B**ridge surface to indicate the case of running on bridge. **8 SM-E** and **7 US-I** denote the summarized results of **8** DOF vehicle running on **S**CR profile of **M**edium span bridge at **E**xternal girder and **7** DOF vehicle running on **U**ER profile of **S**hort span bridge at **I**nternal girder, respectively.

To verify the analytical results of 7 DOF vehicle model, time histories of the vehicle wheel loads at each wheel, RMS values and dominant frequencies of each wheel load are compared with

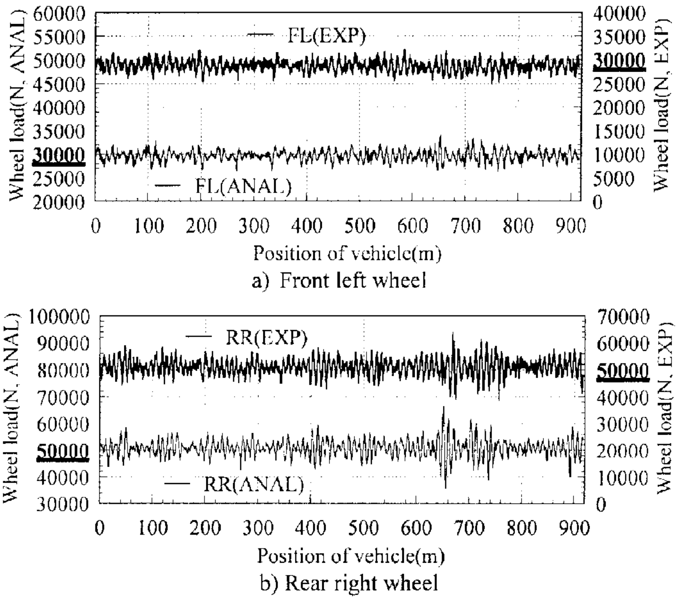

a) Front left wheel

b) Rear right wheel

Fig. 9 Typical time histories of 7 DOF vehicle dynamic wheel load at v = 82.73 km/hr experimental results. During experiment for dynamic wheel loads of the vehicle running on the roadway with SCR profile, the intentioned vehicle speeds were 65 km/hr, 75 km/hr and 85 km/hr but these speeds were measured as 64.96 km/hr, 75.68 km/hr and 82.73 km/hr respectively. The experiment on 7 DOF vehicle and measurement on SCR profile were carried out by Road-Vehicles Research Institute of Netherlands Organization for Applied Scientific Research (TNO). It is possible to see the agreement between analysis and experiment by comparing time histories as shown in Fig. 9.

In the case of 8 DOF vehicle system, experiment was carried out on Umeda Entrance Bridge located at Hanshin Expressway in Osaka, Japan. Fig. 10 shows typical time histories of analytical and experimental results of 8 DOF vehicle running on the steel bridge with UER profile. In addition, Fig. 11 shows typical time histories of strain response of the steel bridge at external girders.

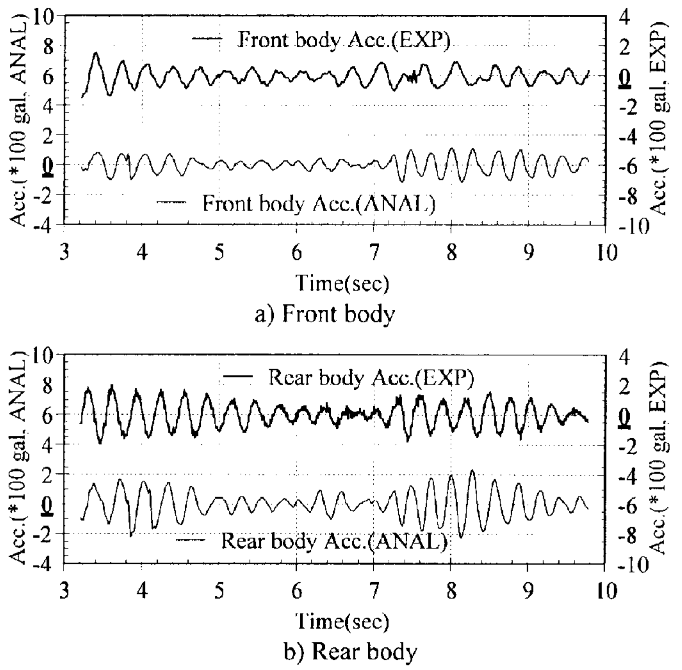

a) Front body

b) Rear body

Fig. 10 Typical time histories of 8 DOF vehicle acceleration at v=17.1 km/hr

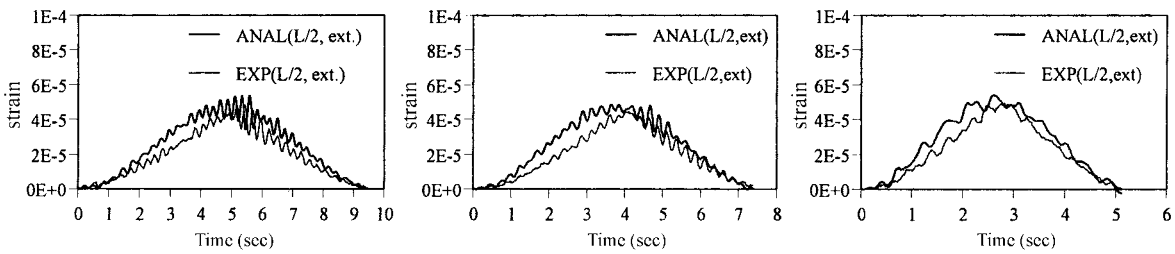

a) External girder (v=17.1 km/hr) b) External girder (v=22.0 km/hr) c) External girder (v=31.7 km/hr)

Fig. 11 Typical time histories of the steel girder bridge response due to 8 DOF vehicle running

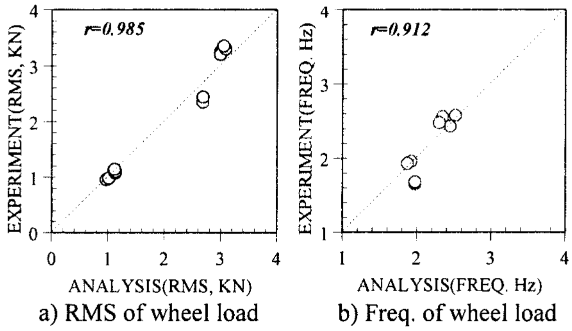

Fig. 12 Co-relation (7 DOF vehicle)

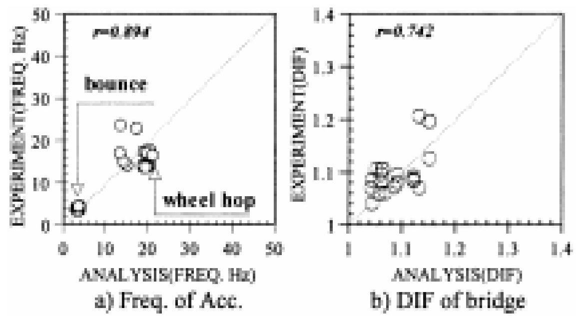

Fig. 13 Co-relation (8 DOF vehicle)

The intentioned vehicle speeds during the experiment were 10 km/hr, 20 km/hr and 30 km/hr, but the measured speeds were 17.1 km/hr, 22.0 km/hr and 31.7 km/hr, respectively. In the case of 8 DOF vehicle running, it is also possible to see the agreement of time histories between those of analysis and experiment.

It is not sufficient, however, to define the validity of analytical results only by comparing the time histories of dynamic wheel load and acceleration. Therefore, in this study, the validity of the analytical results is also verified by comparing the RMS values and dominant frequencies of dynamic wheel loads with experimental ones for 7 DOF vehicle model as summarized in Fig. 12. The r in the figures indicates co-relation coefficient.

To verify the validity of analytical results in 8 DOF vehicle running more clearly, dominant frequencies of acceleration (Fig. 13a), which are taken from accelerometers equipped at vehicle body and axle, are compared with those of analytical results. By using dynamic increment factor (DIF) (Kawatani *et al.* 1993), comparative studies for bridge responses are carried out as shown in Fig. 13b. From those summarized results, it is possible to read the good agreement. Moreover, it can be seen that the analytical time histories of vehicle motions and bridge responses give similar features as measured ones.

Through the comparative study, it is apparent that the analytical results give good agreement with experimental ones, therefore the effectiveness of analytical model encourages practical use. However, in prestressed concrete bridge, there are no measured roadway profile data so that the comparative study has not been carried out.

5. Parametric study

In general, the impact factors taken from in-field bridge test will have features that fluctuate with vehicle speeds. The reason for these phenomena is not clear so far though some research works related to the dynamic amplification factor such as the effect of moving mass on beam (Biggs 1982, Billing 1984 and Cantieni 1984) have been investigated. Because, there are many factors that would affect the bridge-vehicle interaction such as roadway roughness, non-linearity of vehicle suspension system, vehicle axle spacing and frequency spectra of vehicle and bridge as well as moving speed (Cantieni 1992).

As described before, one of the major dynamic loads on the bridge is the dynamic wheel load of the vehicle. Thus it can be concluded that variation of DIF due to different vehicle speeds can be affected by the variation of dynamic wheel loads at different speeds. Therefore, as an example for the parametric study, the effects of vehicle speeds to RMS values of dynamic wheel load and DIF of bridge are investigated. Parametric study is also focused on the effect of different vehicle types and roadway roughness conditions to the variation of RMS values of dynamic wheel loads and DIF of the bridges according to vehicle speed. Those effects to the dominant frequency relations between dynamic wheel loads and bridge responses are also investigated.

5.1 RMS values and dominant frequencies of the dynamic wheel loads of the vehicles running on rigid surface and bridge

To investigate the difference of the dynamic wheel loads between vehicle running on rigid surface and bridge, the co-relations of RMS values as well as dominant frequencies of dynamic wheel load with respect to running condition are considered.

The difference of RMS values of the dynamic wheel load between vehicle running on the bridge and the rigid surface is not clear as shown in Figs. 14a and b, that is there exists strong co-relations. It can also be seen that there are little dominant frequency differences between vehicle running on rigid surface and bridge as shown in Fig. 14c. Fig. 14a indicates the case when 7 DOF vehicle system is running on SCR and UER profile. The co-relation of 8 DOF vehicle system running on SCR and UER profile is shown in Fig. 14b.

The mean RMS values at front and rear wheels of 7 DOF system running on rigid surface and bridge are 0.6 kN and 0.62 kN, respectively. For 8 DOF vehicle system running on rigid surface and bridge, those are 0.62 kN and 0.64 kN, respectively. Accordingly, it can be concluded that RMS values of vehicle passing over the rigid surface are a little greater than RMS values of vehicle running on the bridge. One of the reason for this phenomenon is that a source which activates vehicle motion is not a relative displacement between bridge deformation and roadway roughness but roadway roughness itself, in vehicle running on rigid surface.

5.2 Vehicle speed effects to RMS values of dynamic wheel loads and DIF of bridges

The RMS values of dynamic wheel loads fluctuate with variable vehicle speeds, however they

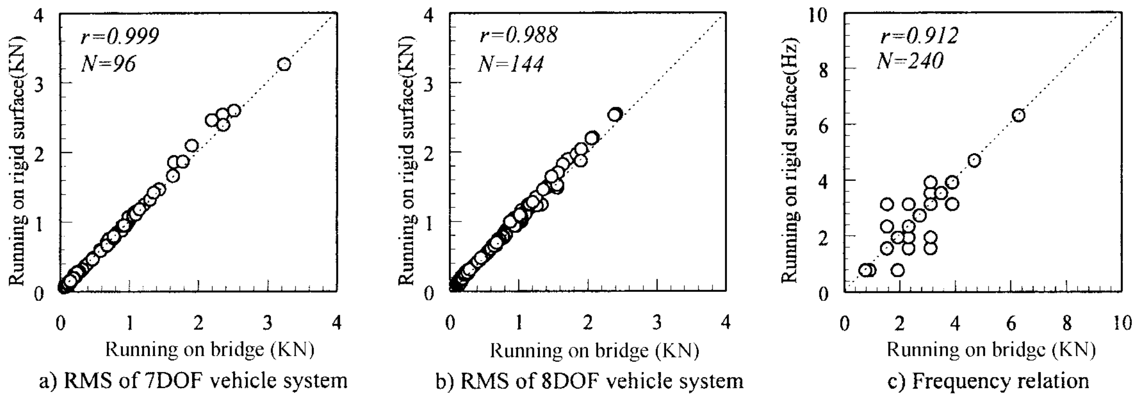

Fig. 14 Relationship between vehicle running on rigid surface and bridge (dynamic wheel loads)

have a tendency to increase with speed as shown in Figs. 15a and b to Figs. 18a and b. But RMS values at the left and right wheels have a little different tendency due to rolling and parallel hop motions. Also it shows that there exists some differences between DIF of the internal and external girders as shown in Fig. 15c to Fig. 18c, which may be affected by external loads occurred at the left and right wheel of the running vehicle. These results can be easily predicted because the dynamic wheel loads at each tire have different magnitude and phase due to different roadway profiles at left and right path. These tendencies necessitate the use of the three-dimensional vehicle model for the bridge-vehicle interaction problem.

The tendency of DIF variation with respect to vehicle speeds (Figs. 15c–18c) is similar to that of RMS values of wheel load (Figs. 15a and b–Figs. 18a and b). It can also be seen that DIF of bridges are strongly affected by surface condition (Fig. 15c vs. Fig. 16c and Fig. 17c vs. Fig. 18c) and vehicle speeds as well as vehicle type or axle spacing (Fig. 15c vs. Fig. 17c and Fig. 16c vs. Fig. 18c).

The co-relation coefficients between RMS values of the dynamic wheel loads and DIF of bridge responses are summarized in Table 3, and it is possible to read a little strong co-relation between RMS values of wheel load and DIF of bridge responses. However those tendency cannot be seen in the case of vehicle running on very smooth roadway (SCR profile). One reason of these phenomena

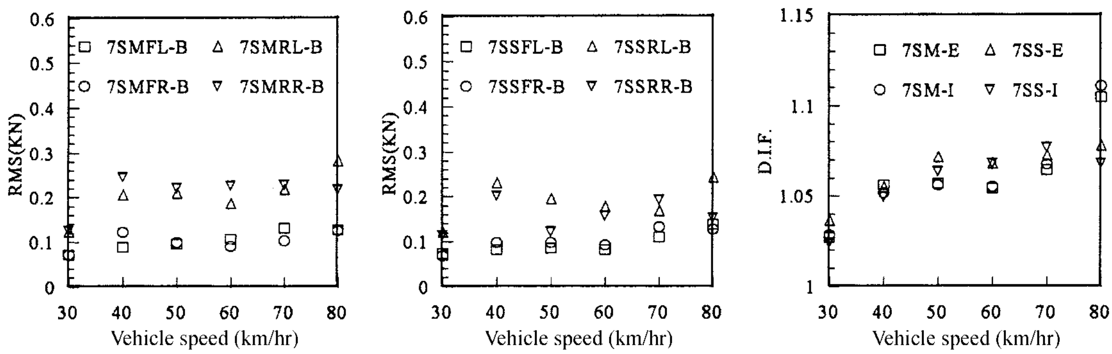

a) Running on medium span BRDG b) Running on short span BRDG c) DIF of girders

Fig. 15 RMS and DIF variation according to vehicle speed (7 DOF, SCR profile)

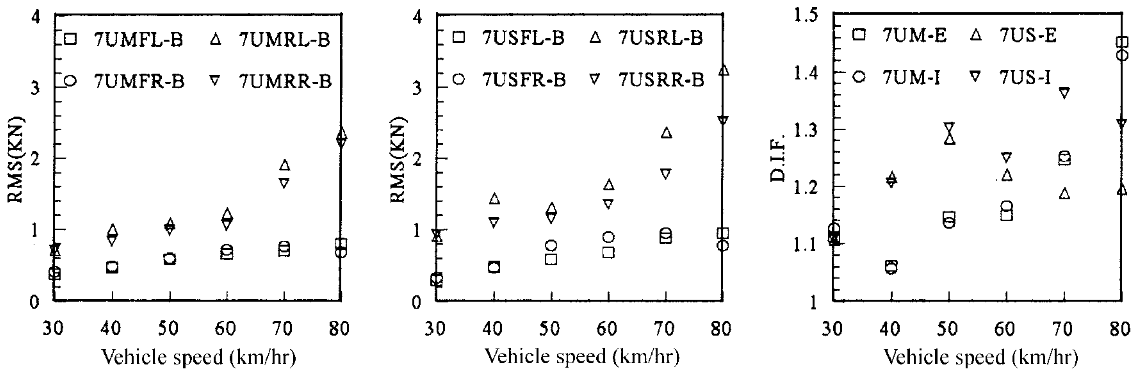

a) Running on medium span BRDG b) Running on short span BRDG c) DIF of girders

Fig. 16 RMS and DIF variation according to vehicle speed (7 DOF, UER profile)

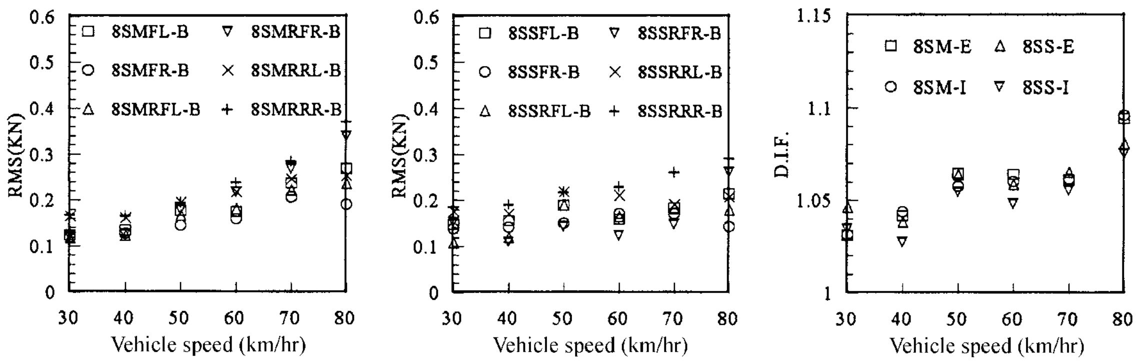

a) Running on medium span BRDG b) Running on short span BRDG c) DIF of girders

Fig. 17 RMS and DIF variation according to vehicle speed (8 DOF, SCR profile)

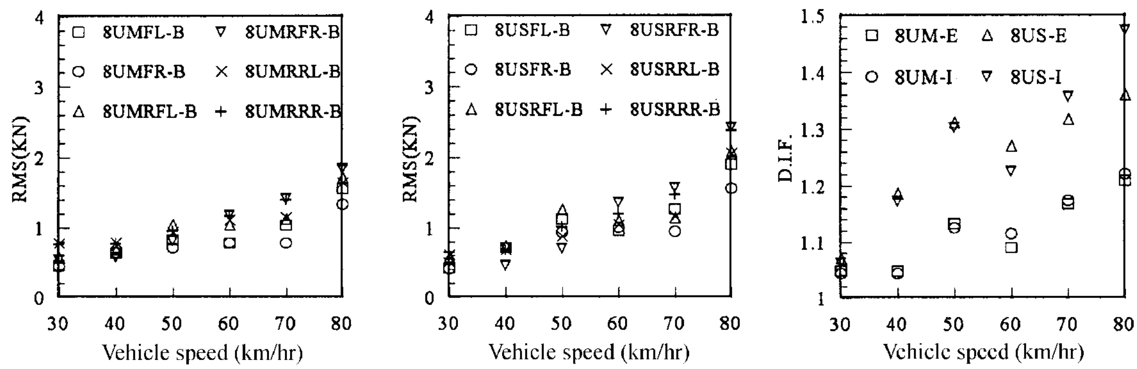

a) Running on medium span BRDG b) Running on short span BRDG c) DIF of girders

Fig. 18 RMS and DIF variation according to vehicle speed (8 DOF, UER profile)

Table 3 Co-relation between RMS values and DIF

		Roadway profile		Vehicle system		Bridge type	
		SCR	UER	7 DOF	8 DOF	Short span	Medium span
Front axle	co-relation coefficient	**0.418**	**0.651**	**0.832**	**0.891**	**0.940**	**0.627**
	(mean of RMS (kN))	(0.135)	(0.775)	(0.370)	(0.542)	(0.483)	(0.428)
Rear axle	co-relation coefficient	**0.587**	**0.692**	**0.870**	**0.823**	**0.835**	**0.861**
	(mean of RMS (kN))	(0.180)	(1.330)	(0.831)	(0.696)	(0.804)	(0.711)
	mean of DIF	1.060	1.202	1.136	1.124	1.150	1.108

may be that the vehicle motion or wheel load cannot fully stimulate the bridge, thus the DIF of the bridge in this case will depend on the fundamental natural frequency or stiffness of bridge itself not on the weak external load. It is possible to read that the DIF of bridge as well as RMS values of dynamic wheel loads are affected by roadway surface condition most severely as expected, from the mean values of the DIF and RMS values in Table 3.

The DIF of the bridges is also affected more seriously by the vehicle with long axle spacing

(7 DOF vehicle system, $\lambda_x = 6.2$ m) than vehicle of short axle spacing (8 DOF vehicle system, $\lambda_x = 3.99$ m). Because the mean RMS value of the dynamic wheel loads at rear axle of the 7 DOF is greater than that of 8 DOF vehicle system despite of its lighter weight. In general, DIF decreases for heavier trucks because the dynamic deflection is similar, while the static deflection is proportional to the truck weight (Kim and Nowak 1995). Of course, the vehicle weight effect to DIF of bridge might also be included because the weight of 8 DOF system is heavier. In addition, the mean DIF of short span bridge is greater than that of medium span bridge as specified in most of countries.

5.3 Vehicle speed effects to dominant frequencies of dynamic wheel loads and bridge responses

Though it is possible to see that the variations of RMS values of the dynamic wheel loads are related with DIF variations of bridge with respect to speed through the research results described here, it is not sufficient to explain the variations of DIF with respect to vehicle speeds. Therefore, it becomes necessary to investigate the dynamic characteristic of the bridge or structure and external loads for further understanding. The dominant frequencies of the wheel loads and bridge responses

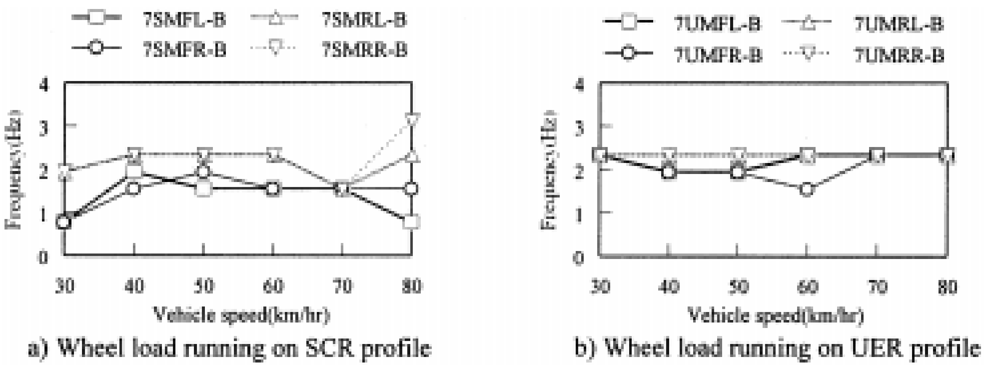

Fig. 19 Dominant frequency variation of 7 DOF vehicle system according to vehicle speed

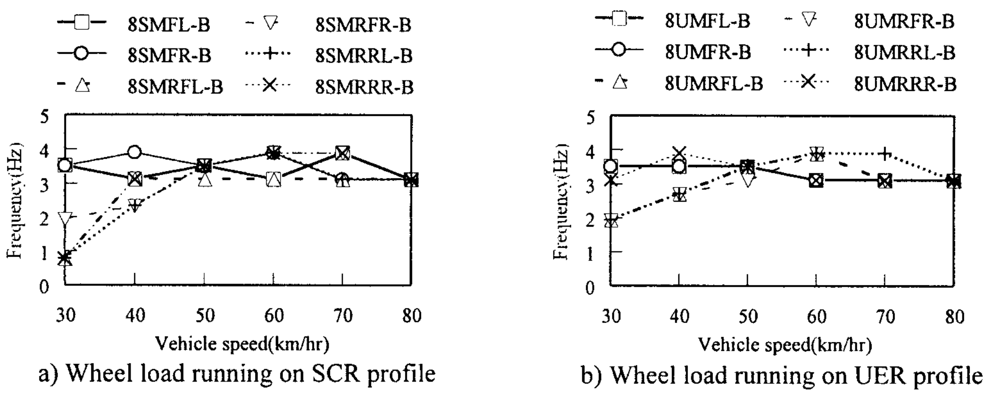

Fig. 20 Dominant frequency variation of 8 DOF vehicle system according to vehicle speed

Table 4. Typical dominant frequencies of vehicle motion in 7 DOF and 8 DOF vehicle systems

Vehicle system	Vehicle body			Front axle		Rear axle		
	bounce	pitching	rolling	parallel hop	tramp	parallel hop	wind up	tramp
7 DOF	2.4	2.4	1.5	11.8	12.3	13.9	–	14.5
8 DOF	3.4	3.6	3.5	17.3	13.9	18.8	17.1	18.3

with respect to speeds are shown in Figs. 19, 20 and 21.

From the figures, it can be seen that the dominant frequencies of dynamic wheel loads of the 7 DOF and 8 DOF vehicles are centered around 2.4 Hz and 3.4 Hz, respectively.

As summarized in Table 4, the dominant frequencies of the bounce motion at each vehicle system are about 2.34 Hz and 3.4 Hz respectively, therefore it is predicted that the dominant frequencies of the wheel loads are located near dominant frequency of the bounce motion.

The dominant frequency variations of the dynamic wheel loads with respect to vehicle speed due to roadway surface conditions are different with each other, as shown in Figs. 19 and 20. That is, in the case of vehicle running on SCR profile, the dominant frequencies are scattered between 0.8 Hz and 3 Hz in 7 DOF vehicle system as shown in Fig. 19a. On the other hand, those frequencies are fluctuated between 1.5 Hz and 2.5 Hz in the case of vehicle running UER profile which have relatively worse surface condition than SCR profile as shown in Fig. 19b.

Those frequency variations of 8 DOF vehicle system running on the SCR profile (Fig. 20a) are scattered between 0.8 Hz and 4 Hz, and between 2 Hz and 4 Hz while the vehicle running on the UER profile as shown in Fig. 20b. One of the reasons that relatively low dominant frequency like 0.8 Hz is shown at low speed may be that the vehicle's dynamic wheel load is not fully activated by smooth roadway roughness input at low speed to generate its frequency feature like bounce motion.

The effect of vehicle speed to dominant frequency of bridge is described in Fig. 21, which shows that the dominant frequencies have tendency to increase according to vehicle speeds. In Fig. 21, the frequencies 2.34 Hz and 3.89 Hz indicate the first and second fundamental natural frequencies of the medium span bridge, respectively. Also, those frequencies 4.69 Hz and 6.65 Hz indicate the first and second fundamental natural frequencies of the short span bridge, respectively.

A remarkable feature in Fig. 21 is that dominant frequencies of short span bridge with fundamental natural frequency of 4.69 Hz due to vehicle running on SCR profile have tendency to

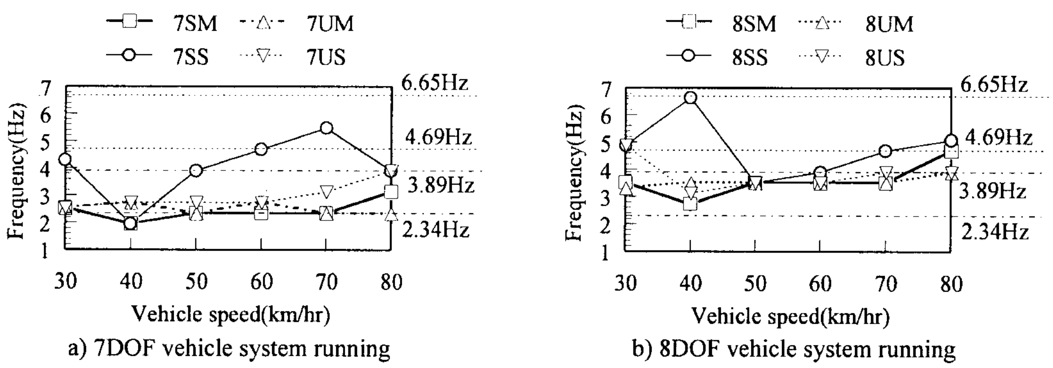

Fig. 21 Dominant frequency variation of bridges according to vehicle speed

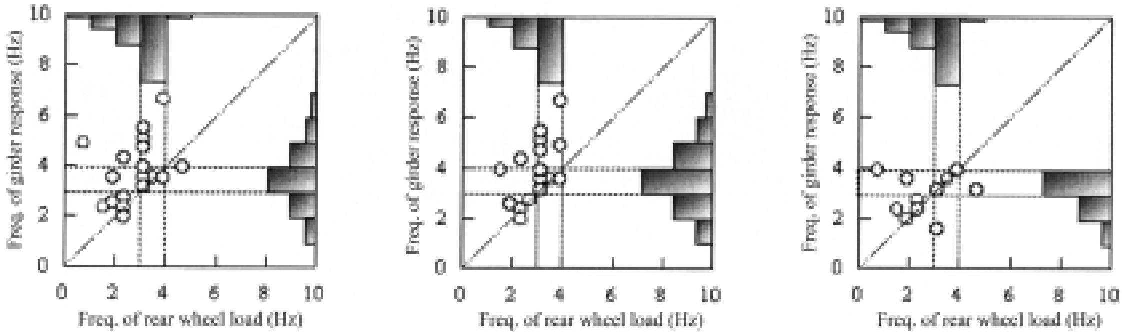

a) Wheel load *vs.* bridge response b) body motion *vs.* bridge response c) Wheel load *vs.* body motion

Fig. 22 Dominant frequency relations (Vehicle running on SCR profile)

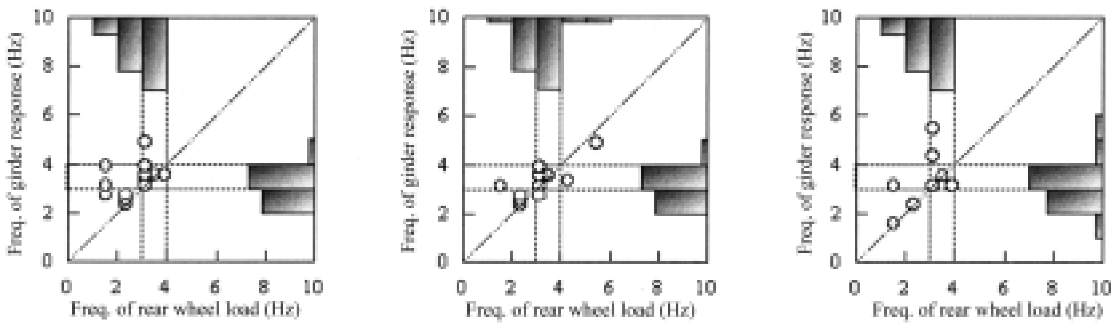

a) Wheel load *vs.* bridge response b) body motion *vs.* bridge response c) Wheel load *vs.* body motion

Fig. 23 Dominant frequency relations (Vehicle running on UER profile)

fluctuate around 4 Hz. On the other hand, those dominant frequencies of the short span bridge with UER profile are scattered around 2.4 Hz, which is similar with vehicle’s dominant frequency. That is, dynamic features of bridge response are dominated by natural frequency of bridge or bridge stiffness itself in the case of vehicle running on very smooth roadway.

Moreover, the dominant frequencies of the bridges are scattered near dominant frequency of bounce motion of the 7 and 8 DOF vehicle systems, that is near 2.4 Hz and 3.4 Hz, except the vehicle running on SCR profile. It supports the results that dynamic characteristic of bridges is dominated by dynamic feature of the vehicle motion or dynamic wheel loads when vehicle is running on the poor roadway, as concluded in section 5.2.

5.4 Frequency relations between dynamic wheel load, vehicle motion and bridge response

Frequency relations between dynamic wheel loads, vehicle motion and bridge responses are shown in Figs. 22 and 23, and the bar graph expresses histogram. From these figures it can be seen that there exist strong resemblance between frequencies of dynamic wheel load, vehicle body motion (bounce motion at each axle) and bridge response. The histogram of frequencies of girder response when vehicle is running on SCR profile (Fig. 22) is dispersed wider than that of vehicle running on UER profile as shown in Fig. 23. It also supports the results that dynamic features of bridge response are dominated not by vehicle motion but by natural frequency of bridge or bridge stiffness itself in the case of vehicle running on very smooth roadway.

Another interesting feature is appeared in Figs. 24 – 29 which show PSD curves of dynamic wheel load and bridge response while 7 DOF vehicle running on SCR and UER profile with different speeds of v=30 km/hr, v=50 km/hr and 70 km/hr. From the figures, it is possible to see that the dominant frequencies of the dynamic wheel load and bridge responses are located near 2.4 Hz.

From these PSD curves, it can be seen that the powers of the wheel load and bridge response are increasing according to vehicle speed. Moreover, those powers of PSD curves increase notably due to roadway roughness conditions. Therefore, it is possible to conclude that the dynamic features of bridge responses can be more easily dominated by dynamic characteristics of vehicle system while vehicle running on rough roadway with high speed than running on smooth roadway with low speed.

Moreover, the peaks of PSD curves of the wheel loads and bridge responses near 14 Hz become apparent with increasing speed. It means that those parallel hop motions with relatively high frequency can affect dynamic wheel loads and bridge responses with increasing speed. In the case of 8 DOF vehicle system, the tendencies are similar with 7 DOF, so that those PSD curves for

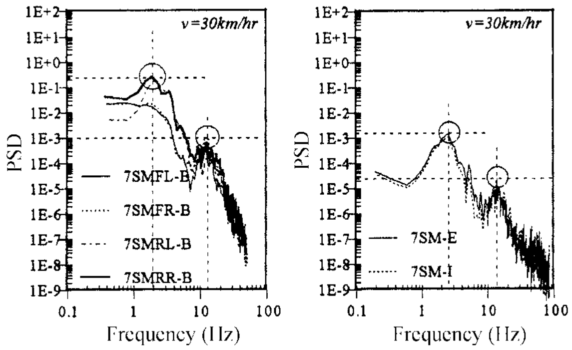

a) Wheel load b) Bridge response

Fig. 24 PSD curves; 7 DOF vehicle running on SCR profile at v=30 km/hr

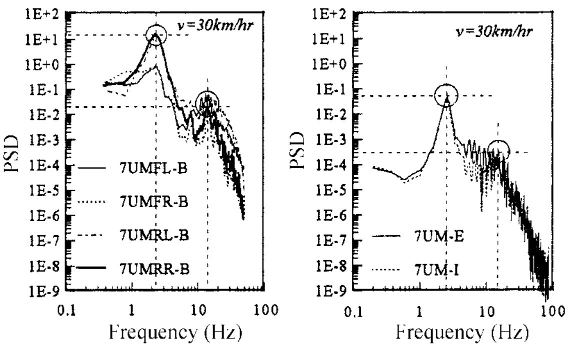

a) Wheel load b) Bridge response

Fig. 25 PSD curves; 7 DOF vehicle running on UER profile at v=30 km/hr

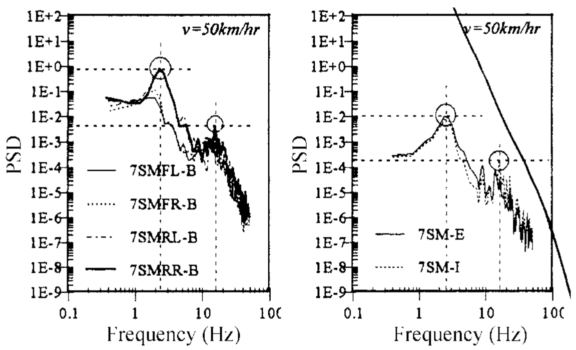

a) Wheel load b) Bridge response

Fig. 26 PSD curves; 7 DOF vehicle running on SCR profile at v=50 km/hr

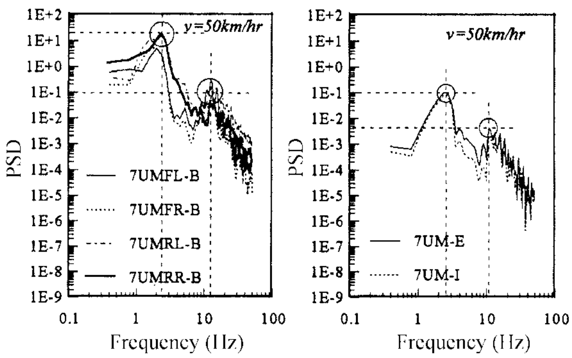

a) Wheel load b) Bridge response

Fig. 27 PSD curves; 7 DOF vehicle running on UER profile at v=50 km/hr

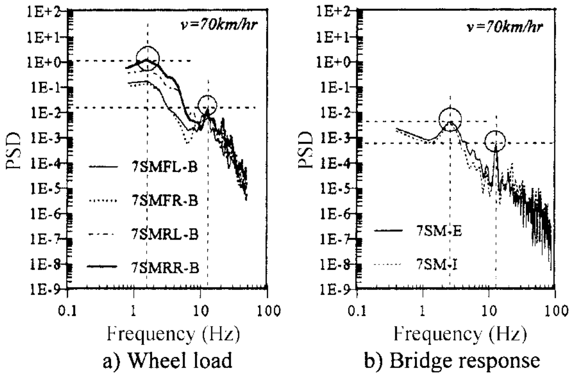

Fig. 28 PSD curves; 7 DOF vehicle running on SCR profile at v=70 km/hr

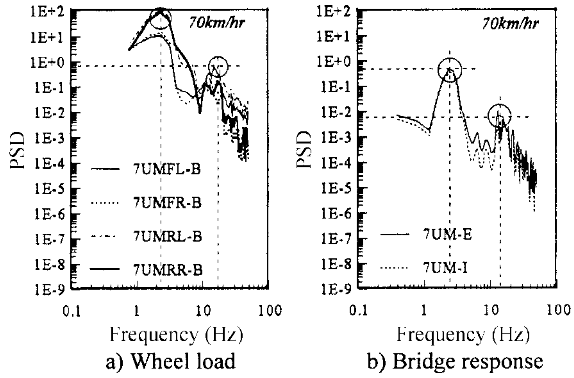

Fig. 29 PSD curves; 7 DOF vehicle running on UER profile at v=70 km/hr

8 DOF are omitted.

6. Conclusions

It is not possible to generalize the vehicle-bridge interaction problems because of its complicate dynamic interaction system. With no relevance to its complicate dynamic relations between vehicle motions and bridge responses with roadway roughness, if some effects of influence factors are defined, it can be seen that the variation is not purely random but must follow certain physical law. Therefore, in this study, to step up a certain physical law of vehicle-bridge interaction problem, computer simulation about dynamic responses of bridges and wheel loads of heavy vehicles idealized as 7 DOF and 8 DOF vehicle system is carried out.

The summarized results can be described as follows;

(1) The validity of the model presented is verified by comparing the analytical results with experimental one, therefore the effectiveness of analytical model encourages practical use.

(2) The RMS values of the dynamic wheel loads fluctuate with vehicle speeds, however they have a tendency to increase with speed. But RMS values at the left and right wheels have a little different tendency due to rolling and parallel hop motions. The difference between RMS values of dynamic wheel loads of the vehicle running on the bridge and on the road is small, but those RMS values of the vehicle passing over the road are a little greater than that of the vehicle running on the bridge.

(3) The DIF of bridges as well as RMS values of dynamic wheel loads are affected by roadway surface condition most severely. The DIF of the bridges is more severely affected by the vehicle with long axle spacing (7 DOF vehicle system) than vehicle of short axle spacing (8 DOF vehicle system). One of the reason may be that the mean RMS value of the dynamic wheel loads at rear axle of the 7 DOF vehicle system is greater than that of 8 DOF vehicle system.

(4) The dynamic features of bridge response are dominated by bridge's natural frequency in the case of vehicle running on smooth roadway, on the other hand, those dynamic features are dominated by vehicle's dynamic features in the case of running on relatively rough roadway which has enough ability to stimulate the vehicles. Moreover, the dominant frequencies of dynamic

wheel load, bounce motion of vehicle and bridge response are strongly related with each other.

(5) Parallel hop motion which has relatively high dominant frequency compared to those of vehicle wheel load and bridge motion can also influence dynamic wheel load and bridge response with increasing speed.

It is noteworthy that there are many factors still left unconsidered related to vehicle-bridge interaction, like the variation of wave frequency input of roadway roughness according to vehicle speed and friction of vehicle suspension system etc. Therefore, as next step for this research, the authors will carry out the parametric studies about vehicle-bridge interactions considering another various factors.

References

Agabein, M.E. (1971), "The effect of various damping assumption on the dynamic response of structures", Bulletin of International Institute of Seismology and Earthquake Engineering, **8**, 217-236.

Biggs, J.M. (1982), "Introduction to structural dynamics", McGraw-Hill, 315-327.

Billing, J.R. (1984), "Dynamic loading and testing of bridges in Ontario", *CSCE J. of Civ. Eng.*, **II**, 833-843.

Cantieni, R. (1984), "Dynamic load testing of highway bridges", *IABSE Proceedings*, P-75/84, 57-72.

Cantieni, R. (1992), "Dynamic behavior of highway bridges under the passage of heavy vehicles", EMPA Report, No.220.

Fafard, M., Mallikarjuna, and Savard, M. (1993), "Dynamics of bridge-vehicle interactions", *Proc. of Structural Dyanmics-EURODYN'93*, 951-960.

Huang, T. (1976), "Vibration of bridges", *Shock Vibr., Dig.*, **8**, 61-76.

Inbahathan, M.J., and Wieland, M. (1987), "Bridge vibrations due to vehicle moving over rough surface", *J. Struct. Eng.*, ASCE, **113**(9), 1994-2008.

ISO (1972), "Proposals for generalized road inputs to vehicles", ISO/DIS2631, 1-7.

Kawatani, M., Nishiyama, S., and Yamada, Y. (1993), "Dynamic response analysis of highway bridges under moving vehicle", Technical Report of the Osaka Univ., **43**(2137), 109-118.

Kawatani, M., and Kim, C.W. (1998), "Effects of gap at expansion joint on traffic-induced vibration of highway bridge", *CSCE Proc. of Developments in Short and Medium Span Bridge Engineering'98*, **I**, 285-294.

Kim, S., and Nowak, A.S. (1995), "Load distribution and impact factors for I-girder bridges", *ASCE J. Bridge Eng.*, **2**(3), 97-104.

Mulcathy, N.L. (1983), "Bridge response with tractor-trailer vehicle loading", *Earthq. Eng. and Struct. Dyn.*, **11**, 649-665.

Nassif, H.N., and Nowak, A.S. (1995), "Dynamic load spectra for girder bridge", Transportation Research Record, 1476, 69-83.

Page, J. (1976), "Dynamic wheel load measurements on motorway bridges", TRRL Laboratory Report 722.

Yang, Y.B., Yau, J.D., and Hsu, L.C. (1997), "Vibration of simple beams due to trains moving at high speeds", *Eng. Struct.*, **19**(11), 936-944.

Zienkiwicz, O.C., and Taylor, R.L. (1991), *The Finite Element Method*, McGraw-Hill, **1, 2**.